Research by statistical methods of models of the function of transformation of optical circuits of the means of measuring the temperature based on the effect of Raman

Yurii Kryvenchuk[0000-0002-2504-5833], Iryna Shvorob[0000-0001-5569-2647], Yurii Novytskyi[0000-0002-5011-7034], Yevgen Zasoba [0000-0003-4830-8306], Yaroslav Matviychuk [0000-0002-5570-182X], Vladyslav Mykhailyshyn [0000-0003-1889-9053], Nataliya Hrabovs'ka [0000-0002-5032-2257], Nataliia Topylko [0000-0002-3200-3391], Mykhailo Osypov [0000-0002-6611-724X], Hrystyna Yakymyshyn [0000-0002-8772-0101]

Lviv Polytechnic National University, Lviv 79013, Ukraine
yurkokryvenchuk@gmail.com, iryna.b.shvorob@lpnu.ua, yuranov_lpnu@ukr.net, geka.zasoba@gmail.com, matv@ua.fm, vladyslavmykhailyshyn@gmail.com, natahagr@gmail.com, topnatlviv@gmail.com, mykhailo.osypov@gmail.com, yakymyshyn_hrystyna@ukr.net

Abstract. Industry 4.0 continually flows into the daily technical life of the world. Germany has created the platform Industry 4.0. Like the Germans, France launched the initiative, also at the state level. India, China and the United States have strong initiatives. The new concept makes it possible to speed up the production of various parts and entire products by two, and sometimes by three times. For such purposes, it is not only necessary to use fast data transfer protocols, but also to develop new sensors that will perform such fast and accurate work. As a rule, the most controlled parameter in the industry is temperature, meaning such high-precision thermometric sensors need to be verified to confirm their metrological characteristics. For this purpose, the most optimal method is the Raman scattering. In order to confirm the accuracy of metrological verification, it is important to know the errors of the conversion function of optical circuits, since this entails an increase in the relative mean-rms deviation of the equivalent frequency of the anti-Stokes component of the spectrum, which in turn directly affects the accuracy of determining the temperature and metrology.

Keywords: Industry 4.0, Temperature measurement, Raman spectrum, Raman thermometer, Mathematical model

1 Introduction

In [1], the synthesis of models of functions of transformation of optical elements and optical circuits of the means of measuring the temperature and spectra of the Raman was performed. These models allow us to investigate the dependence of the relative

 CybHyg-2019: International Workshop on Cyber Hygiene, Kyiv, Ukraine, November 30, 2019.

root mean square deviation of the equivalent frequency of the anti-Stokes component of the Raman spectrum for different spectral models and under the influence of different error components at different spectral analyzer resolutions. It is also possible to determine the best method for determining the equivalent frequency of the anti-Stokes component of the Raman spectrum. These studies allow us to improve the metrological characteristics of temperature measuring instruments that will be used for metrological verification of temperature sensors in the industry. The results can also be used to determine the lack of parts on the production line.

2 State of arts

Analyzing optical circles and optical elements, it is determined that, as a rule, for each specific task, they use specific optical circuits, since the objects under study are of different shapes and sizes, and may also simply be located at different points. However, there are five of the most widely used optical circuits worth converting. Each circuit has its own characteristics due to a different set of optical elements that will distort the original spectrum, and as a consequence contribute to the error of temperature measurement by this method. Matlab modeled secondary circuits of optical circuits and input spectra of Raman scattering. The following parameters were investigated at the input: the linear, nonlinear components of the error model of the optical element re-creation function is 2%, the methods of determining the equivalent frequency of the anti-stokes component of the Raman spectrum: the center of mass method and the median method. The resolution of the spectrum analyzer at a frequency of 1 ... 10 cm-1, the forms of simulated spectra for the study: rectangular, triangular, trapezoidal, sawtooth. The number of bones of random sequences is one thousand. At the output we obtain the following results: the best method for determining the equivalent frequency of the anti-stokes component of the Raman spectrum, the dependence of the relative mean-rms deviation of the equivalent frequency of the anti-stokes component of the Raman spectrum on the frequency resolution of the analyzer. Uncertainty of determining the equivalent frequency of the anti-stokes component of the Raman spectrum from the forms of simulated signals, the influence of linear, nonlinear, total error of the transmitting characteristics of optical elements.

The term "Industry 4.0" was created for the anticipated "fourth industrial revolution". Accordingly, Industry 4.0 means in-depth digitization in industrial enterprises in the form of a combination of Internet technologies with future-oriented technologies in the field of "smart" objects (machines and products). This transforms industrial production systems so that products control their own production process. The importance of digitalization and the Internet is also reflected in discussions of related concepts such as the Internet of Things or the Industrial Internet. Industry 4.0 is initiated not by a single technology, but by the interaction of several technological objects whose quantitative consequences together create new ways of production. The main advantage over the technological perspective is the ability to facilitate tasks that previously required heavy manual work, such as high-precision methods of temperature measurement.

Scientific and technological progress is closely linked to the improvement of measuring equipment. This is completely true of thermometry, which is constantly evolving. The measurement range is being expanded, new methods and temperature measurement tools are being developed to provide their required metro-logical characteristics, since the accuracy of maintaining the temperature regime in most technological processes is the main parameter on which the quality of the final product depends. Open source obtained quantitative and spatially differentiated temperature data available for thermal actuator designs using MEMS. The lion's cup of modern MEMS has become tiny in size. In the process of manufacturing such miniature sensors, a large number of parameters must be controlled and the most controlled parameter is the temperature. The results obtained from experimental measurements of the temperature profile for bending type actuators can be used to validate existing models, but do not allow us to determine the optimal model. Applying artificial intelligence technologies and Big Data concepts to control temperature and analyze the data obtained will minimize the output of the defect. Automation facility (Joint Ukrainian-German company "Spheros-Electron") defects details that have deviations from geometric parameters and / or metallurgical defects. The minimization of metallurgical defects was the most difficult and interesting task for technologists. The "responsible" for them was the installation of controlled cooling, since the main causes of such defects - uneven cooling and violations of temperature. It has become an "optimization point".

3 Materials and Methods

The uncertainty dependence of the determination of the equivalent frequency of the anti-stokes components of the Raman spectrum of frequency resolution is taken into account for the linear, nonlinear and random components of the error of the Monte Carlo optical circuit conversion function for the five most commonly used spectra of the common optical circuits in the process of obtaining the spectrum.

Finding the dependence of the uncertainty of determining the frequency shift of the CRC on the frequency resolution for the test signal with a random component of the error of the transmission characteristic of the elements of the optical circuit, linear and nonlinear component of the error works according to the following algorithm.

1) Data entry is made, and then, based on the number of frequency resolution values, minimum and maximum frequency resolutions, the resolution step of the spectrometer is formed. This will allow you to select the most optimal frequency analyzer.

2) A spectrum model of a known shape is generated, which alternately falls on the optical elements of the secondary circuit of the optical circuit, where there is actually a multiplication of the complex frequency characteristics of the optical elements of the secondary circuit of the optical circuit with random linear, nonlinear components of the error of the optical elements and spectrum. Such operation is performed n-number of times and from each spectrum the equivalent frequency of the anti-Stokes component of the Raman spectrum is determined by the median and the center of mass method.

3) The mathematical expectation, variance and root mean square deviation and uncertainty of the equivalent frequency of the anti-stokes component of the Raman spectrum are determined by the two methods mentioned above.

The Matlab code snippet for steps 1-2 is shown below:

```
x= Vmin:delta_V(j):Vmax;
y1 = trapmf(x,[410 430 430 450]);
y2 = trapmf(x,[400 450 650 800]);
y3 = trapmf(x,[400 450 650 800]);
y_4 = trapmf(x,[523 523 541 541]);
y4=(y_4*(-1)+abs(max(y_4)));
y6 = trapmf(x,[400 424 662 700]);
    for k = 1:100;
      K_1_poxubka_Linse = double(rand(1)-0.5)*2*K_1_diviation_Linse;
        if K_polinom_linse1 == 1
        pRange_1 = polyfit([x(1), x(end)], [0,K_1_poxubka_Linse], K_polinom_linse1);  % Random line
        elseif K_polinom_linse1 == 2
        pRange_1 = polyfit([x(1), x(round(length(x)/2)), x(end)], [0,K_1_poxubka_Linse, 0], K_polinom_linse1);
        end
      yRange_1 = polyval(pRange_1,x);
      yRandom = K_1_poxubka_Linse_random*(rand(size(yRange_1))-0.5)*2;  % Random
      yLinse_1 = y2+yRange_1+yRandom; % summary Random

      K_2_poxubka_Linse = double(rand(1)-0.5)*2*K_2_diviation_Linse;
        if K_polinom_linse2 == 1
        pRange_2 = polyfit([x(1), x(end)], [0,K_2_poxubka_Linse], K_polinom_linse2);
        elseif K_polinom_linse2 == 2
        pRange_2 = polyfit([x(1), x(round(length(x)/2)), x(end)], [0,K_2_poxubka_Linse, 0], K_polinom_linse2);
        end
      yRange_2 = polyval(pRange_2,x);
      yRandom = K_2_poxubka_Linse_random*(rand(size(yRange_2))-0.5)*2;
      yLinse_2 = y3+yRange_2 +yRandom; % summary Random

      K_1_poxubka_NF = double(rand(1)-0.5)*2*K_1_diviation_NF;
        if K_polinom_NF == 1
        pRange_3 = polyfit([x(1), x(end)], [0,K_1_poxubka_NF], K_polinom_NF);
        elseif K_polinom_NF == 2
        pRange_3 = polyfit([x(1), x(round(length(x)/2)), x(end)], [0,K_1_poxubka_NF, 0], K_polinom_NF);  % Random line
        end
      yRange_3 = polyval(pRange_3,x);
```

```
        yRandom = K_1_poxubka_NF_random*(rand(size(yRange_3))-0.5)*2;    %
Random
        yNF = (yRange_1+y4+yRandom); % summary Random

        K_poxubka_Lambda = double(rand(1)-0.5)*2*K_2_diviation_Lambda;
          if K_polinom_Lambda == 1
          pRange_5     =     polyfit([x(1),     x(end)],     [0,K_poxubka_Lambda],
K_polinom_Lambda);  % Random line
          elseif K_polinom_Lambda == 2
          pRange_5     =     polyfit([x(1),     x(round(length(x)/2)),     x(end)],
[0,K_poxubka_Lambda, 0], K_polinom_Lambda);
          end
        yRange_5 = polyval(pRange_5,x);
        yRandom = K_poxubka_Lambda_random*(rand(size(yRange_5))-0.5)*2;   %
Random
        yLambda = y6 +yRange_5+yRandom; % summary Random

        y = (y1.* yLinse_1.* yLinse_2.* yNF.*yLambda);
        GC_x(k) = sum(x.*y)/sum(y);
        GC_y(k) = sum(x.*y)/sum(x);
        [M_y(k),indMax]=max(y);% maximum stocks
        SquareY = cumsum(y);
        indexSqR_1 = length(y(SquareY <= sum(y)/2));% index of half square ratio
        indexSqR_2 = indexSqR_1 +1;
        x_1 = x(indexSqR_1);
        x_2 = x(indexSqR_2);
        y_1 = SquareY(indexSqR_1);
        y_2 = SquareY(indexSqR_2);
        SqR_y(k) = sum(y)/2;
        SqR_x(k) = x_1 + (SqR_y(k)-y_1)/(y_2-y_1)*(x_2-x_1);
        M_x(k)=x(indMax);
      end
```

4 Experiment

Figure 1 shows the structure of the secondary circuit of the optical circuit of a temperature measuring instrument with a notch filter.

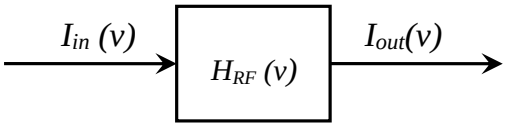

Fig. 1. The structure of the secondary circuit of the optical circuit of the temperature measuring instrument with a notch filter

The function of converting the secondary circle of the optical circuit is described by the expression:

$$I_{out}(\nu) = I_{in}(\nu) \cdot \left| H_{RF}(\nu) \right|^2 \quad (1)$$

Figures 2 show the dependences of the relative root mean square deviation of the equivalent frequency value of the anti-Stokes component of the Raman spectrum for the corresponding rectangular, trapezoidal, triangular and saw tooth models of the Raman spectra at linear, nonlinear and total error of the error the ability of the analyzer at frequency 1 and 10 cm-1.

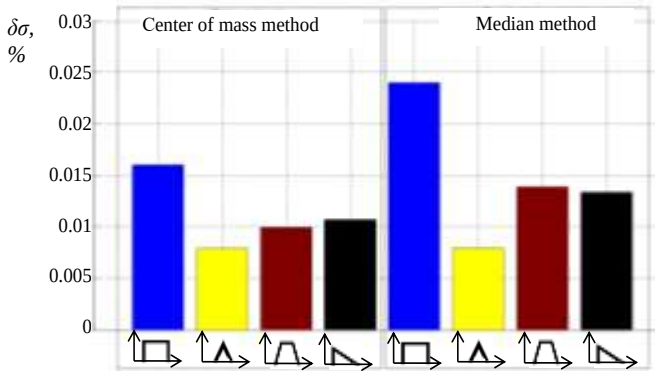

Fig. 2. Dependences of the relative root mean square deviation of the equivalent frequency value of the anti-Stokes component of the Raman spectrum for different spectral models and the linear error component of the conversion function of the optical circuit elements at 1 cm^{-1} resolution

The study was performed under the following parameters: frequency band of the filter filter from 1890 to 1869 cm-1, laser wavelength 532 nm. The linear, nonlinear components of the error model of the optical element conversion function is 2%.

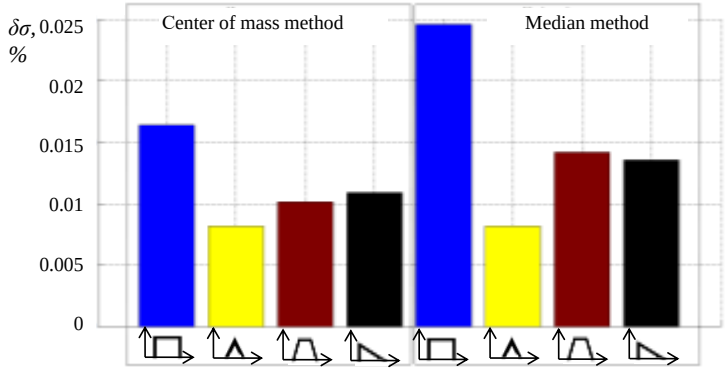

Fig. 3. Dependences of the relative standard deviation of the equivalent frequency value of the anti-Stokes component of the Raman spectrum for different spectral models and the linear error component of the conversion function of the elements of the optical scheme at a resolution of 10 cm^{-1}

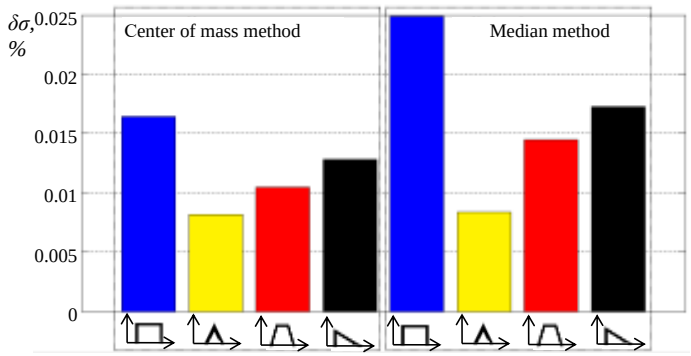

Fig. 4. Dependences of the relative root mean square deviation of the equivalent frequency value of anti-Stokes component of the Raman spectrum for different spectral models and nonlinear component of the error of the conversion function of the elements of optical scheme at resolution of 1 cm^{-1}

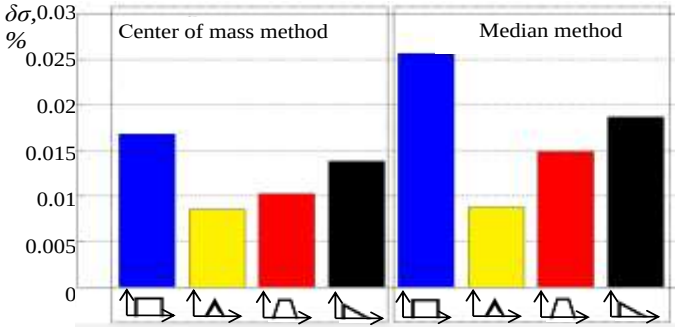

Fig. 5. Dependencies of the relative root mean square deviation of the equivalent frequency value of the anti-Stokes component of the Raman spectrum for different spectral models and the nonlinear component of the error of the optical circuit conversion function at a resolution of 10 cm^{-1}

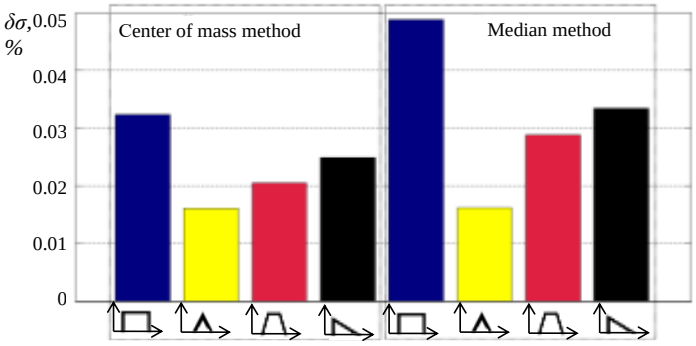

Fig. 6. Dependences of the relative root mean square deviation of the equivalent frequency value of the anti-Stokes component of the Raman spectrum for different spectral models and the total error of the conversion function of the elements of the optical scheme at a resolution of 1 cm^{-1}

Studies have shown that for a rectangular model of the Raman spectrum under the influence of a linear component of the error of the relative standard deviation of the determination of the equivalent frequency of the anti-stokes component of the spec-

trum of Raman by the center of mass for the resolution of the spectrometer 1 cm^{-1} the relative rms of the spectrum % (Figure 2), when exposed to a nonlinear asymmetric component of error 0.0164% (Figure 4), and the total level of accuracy - 0.0168% (Figure 6).

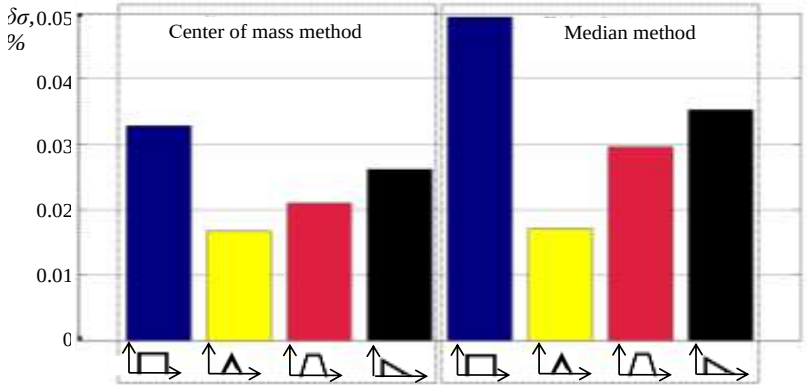

Fig. 7. Dependences of the relative root mean square deviation of the equivalent frequency value of the anti-Stokes component of the Raman spectrum for different spectral models and the total error of the optical circuit conversion function at a resolution of 10 cm^{-1}

For the linear component of error, it is 0.0024% (Figure 2), for the nonlinear component of error - 0.0025% (Figure 4), and for the total error - 0.0049% (Figure 6).

Figure 8 shows the structure of the secondary circuit of the optical circuit of the flame temperature measuring device.

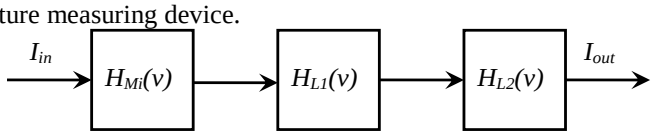

Fig. 8. Structure of the secondary circuit of the optical circuit of the flame temperature measuring device

The function of transformation of the secondary circle of the optical circuit (Figure 8) is described by the expression:

$$I_{out}(\nu) = I_{in}(\nu) \cdot \left|H_{L1}(\nu)\right|^2 \cdot \left|H_{L2}(\nu)\right|^2 \cdot \left|H_{Mi}(\nu)\right|^2 \qquad (2)$$

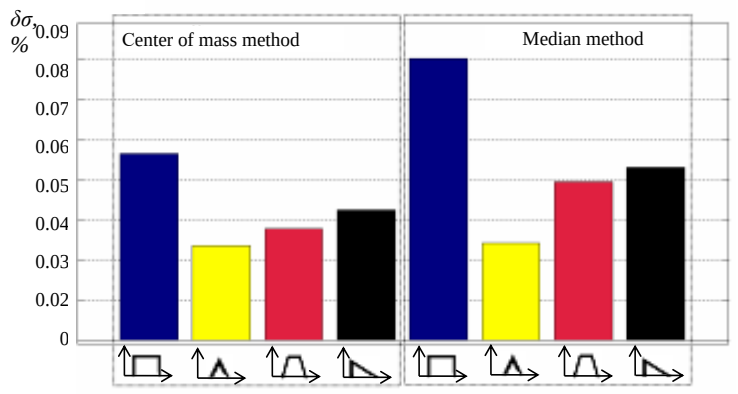

Fig. 9. Dependences of the relative standard deviation of the equivalent frequency value of the anti-Stokes component of the Raman spectrum for different spectral models and the total error of the conversion function of the elements of the optical scheme at a resolution of 1 cm^{-1}

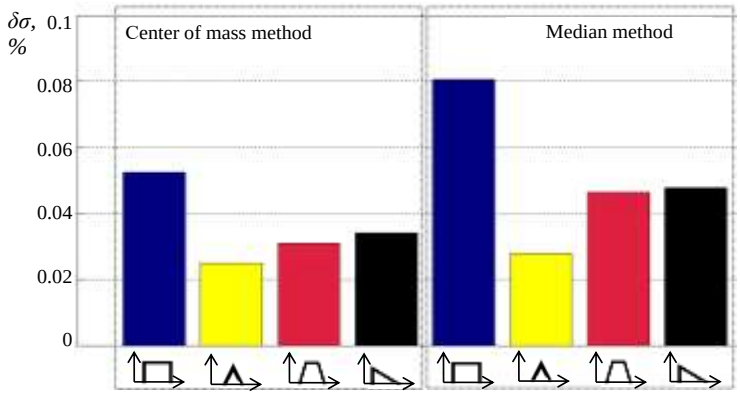

Fig. 10. Dependences of the relative root mean square deviation of the equivalent frequency value of the anti-Stokes component of the Raman spectrum for different spectral models and the total error of the optical circuit conversion function at a resolution of 10 cm^{-1}

Figures 9 - 10 show the dependences of the relative root mean square deviation of the equivalent frequency of the anti-Stokes component of the Raman spectrum for the corresponding, rectangular, trapezoidal, triangular and saw tooth models of Raman spectra at the total error of the transform function of the optical function.

Figure 11 shows the structure of the secondary circuit of the optical circuit of the temperature measuring tool using a prism and narrow band filter.

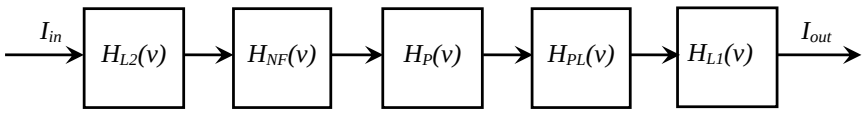

Fig. 11. Structure of the secondary circuit of the optical circuit of the temperature measuring tool using a prism and narrow band filter

The function of converting the secondary circle of the optical circuit (Figure 11) is described by the expression:

$$I_{out}(\nu) = I_{in}(\nu) \cdot \left|H_{L1}(\nu)\right|^2 \cdot \left|H_{L2}(\nu)\right|^2 \cdot \left|H_P(\nu)\right|^2 \cdot \left|H_{NF}(\nu)\right|^2 \cdot \left|H_{PL}(\nu)\right|^2 \qquad (3)$$

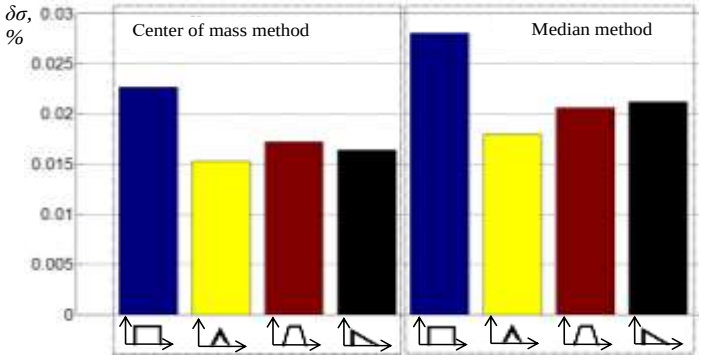

Fig. 12. Dependences of the relative root mean square deviation of the equivalent frequency value of the anti-Stokes component of the Raman spectrum for different spectral models and the total error of the optical circuit conversion function at a resolution of 1 cm^{-1}

Figures 12 -13 show the dependences of the relative root mean square deviation of the equivalent frequency value of the anti-Stokes component of the spectrum for the corresponding rectangular, trapezoidal, triangular and saw-like models of Raman spectra at the total error of the conversion function of the optical circuit elements.

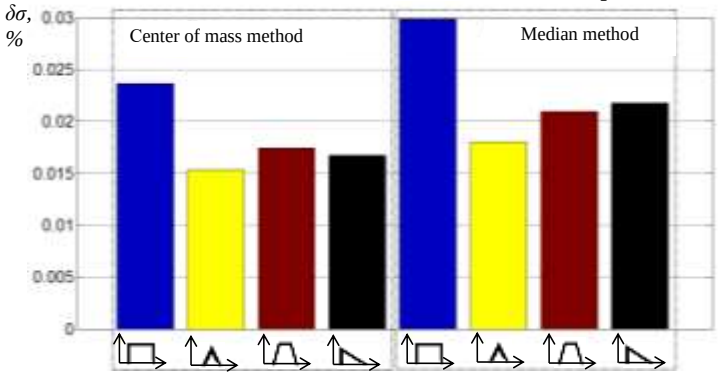

Fig. 13. Dependences of the relative root mean square deviation of the equivalent frequency value of the anti-Stokes component of the Raman spectrum for different spectral models and the total error of the optical circuit conversion function at a resolution of 10 cm^{-1}

The study was performed under the following parameters: frequency band of the harvesting lens from 1428 to 2500 cm^{-1}, frequency band of the filter filter from 1890 to 1869 cm^{-1}, step by frequency 1 and 10 cm^{-1}.

Figure 14 shows the structure of the secondary circle of the optical circuit for temperature measurement using a microscope and aperture.

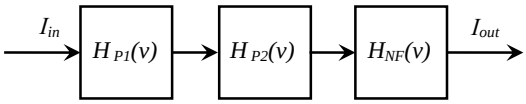

Fig. 14. Structure of the secondary circuit of the optical circuit of the temperature measuring tool using a microscope and aperture

The function of transformation of the secondary circle of the optical circuit (figure 14) is described by the expression:

$$I_{out}(\nu) = I_{in}(\nu) \cdot \left|H_{P1}(\nu)\right|^2 \cdot \left|H_{P2}(\nu)\right|^2 \cdot \left|H_{NF}(\nu)\right|^2 \quad (4)$$

Figures 15-16 show the dependences of the relative root mean square deviation of the equivalent frequency value of the antistatic component of the spectrum for the corresponding rectangular, trapezoidal, triangular and saw tooth models of Raman spectra at the total error of the conversion function of the element of the transformation function. The pre-survey was performed under the following parameters: frequency band of the filter filter from 1890 1869 cm^{-1}, step at frequency 1 and 10 cm^{-1}.

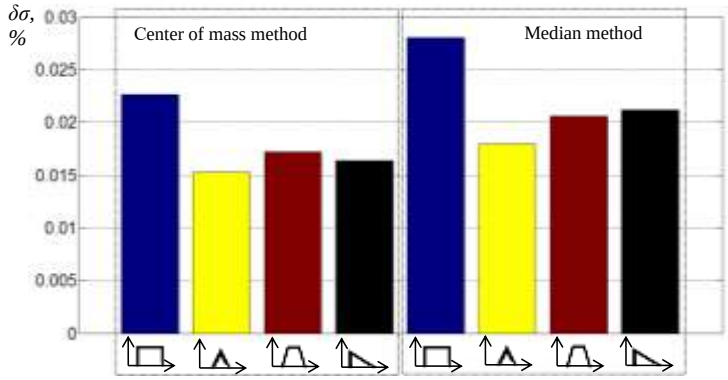

Fig. 15. Dependences of the relative standard deviation of the equivalent frequency value of the anti-Stokes component of the Raman spectrum for different spectral models and the total error of the conversion function of elements of optical scheme at resolution of 1 cm^{-1}

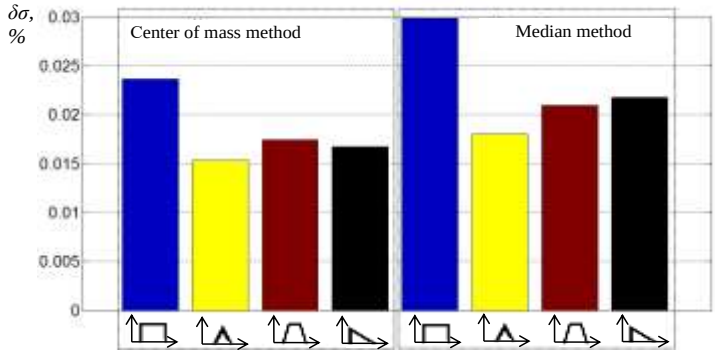

Fig. 16. Dependences of the relative root mean square deviation of the equivalent frequency value of the anti-Stokes component of the Raman spectrum for different spectral models and the total error of the optical circuit conversion function at a resolution of 10 cm^{-1}

A block diagram of a temperature measuring instrument with a notch filter and a polarizer is shown in figure 17.

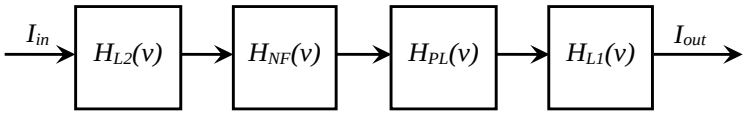

Fig. 17. Structural optical diagram of a temperature measuring instrument with a notch filter and a polarizer

The secondary circuit conversion function of the optical circuit is of the form:

$$I_{out}(\nu) = I_{in}(\nu) \cdot \left|H_{L1}(\nu)\right|^2 \cdot \left|H_{LP2}(\nu)\right|^2 \cdot \left|H_{NF}(\nu)\right|^2 \cdot \left|H_{PL}(\nu)\right|^2 \quad (5)$$

Figures 18-19 presents the dependences of the relative root mean square deviation of the value of the equivalent frequency of the anti-Stokes component of the spectrum for the corresponding rectangular, trapezoidal, triangular and saw tooth models of the Raman spectra of the combined error of the transform element.

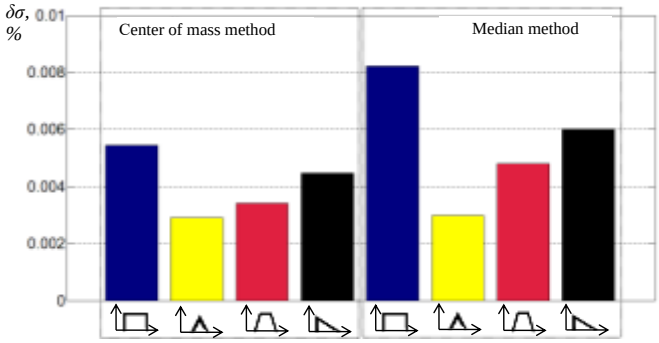

Fig. 18. Dependences of the relative root mean square deviation of the equivalent frequency value of the anti-Stokes component of the Raman spectrum for different spectral models and the total error of the conversion function of the optical circuit elements at a resolution of 1 cm^{-1}

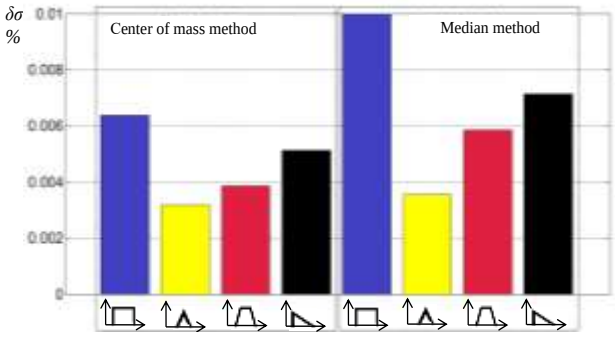

Fig. 19. Dependences of the relative root mean square deviation of the equivalent frequency value of the anti-Stokes component of the Raman spectrum for different spectral models and the total error of the optical circuit conversion function at a resolution of 10 cm^{-1}

The study was performed under the following parameters: frequency band of the harvesting lens from 1428 to 2500 cm^{-1}, frequency band of the filter filter from 1890 1869 cm^{-1}, polarizer with coordinates 1428, 1620, 2237, 2500 cm^{-1}, step in frequency 1 and 10 cm^{-1}.

5 Conclusions

Studies have shown that under the influence of the model total error of the function of conversion of optical elements for all optical circuits, the studied models of the Raman spectra, taking into account the minimum dependence of the relative standard deviation of the equivalent frequency of the anti-stokes component of the spectrum of Raman provides the center of mass. Figure 19 presents the results of the study of the dependence of the relative standard deviation of the equivalent frequency of the anti-Stokes component of the Raman spectrum on the frequency resolution of the spectrum analyzer, taking into account the total error of the elements of the optical circuit, which is 2%. The limit value of the error of temperature measurement by means based on the effect of CRC takes the following form:

$$\delta T = \delta_m + \delta_{pc} + \delta_{sc} + {}_{sa} = 0{,}04 + 0{,}00008 + 0{,}02 + 0{,}09 \approx 0{,}15\% \qquad (6)$$

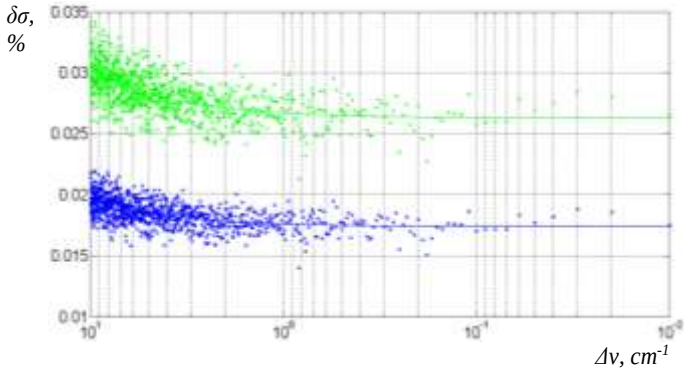

Fig. 20. Dependences of the relative root mean square deviation of the equivalent frequency value of the anti-Stokes component of the Raman spectrum on the resolution of the frequency of the analyzer when exposed to a total error

The obtained research results (figure 19) showed that there is a certain value of the resolution of the spectrum analyzer at a frequency whose decrease practically does not reduce the dependence of the relative mean-square deviation of the value of the equivalent frequency of the anti-Stokes component of the Raman spectrum. For example, for a resolution of less than 1 cm^{-1}, the dependence of the relative standard deviation of the equivalent frequency of the anti-Stokes component of the Raman spectrum is practically unchanged and is approximately 0.00083% for the center of mass method and 0.00126% for the median method of determination the equivalent frequency of the anti-Stokes component of the Raman spectrum.

The results obtained (Figure 19) allow for the required relative root-mean-square deviation of the equivalent frequency of the anti-stokes component of the Raman

spectrum to impose requirements on the metrological and technical characteristics of the analyzer or to estimate the relative relative error of determining the equivalent frequency of the anticancer spectrum - nightly characteristics of the analyzer.

The work was implemented during the implementation of an economic agreement for Spheros-Elektron, Lviv, as an element of the Industrial Internet of Things in Industry 4.0. Consequently, studies have shown that the center of mass method is optimal for determining the equivalent frequency of the anti-Stokes component of the Raman spectrum. Its use ensures a minimum confidence relative error in the determination of the equivalent frequency of the anti-Stokes component of the Raman spectrum compared to other methods. The dependence of the value of the equivalent frequency of the anti-Stokes component of the Raman spectrum on the laser radiation intensity is investigated and it is found that the change in the intensity of the laser beam does not affect the error in determining the equivalent frequency of the anti-stokes component of the Raman spectrum. The dependence of the relative root mean square deviation of the value of the equivalent frequency of the anti-Stokes component of the Raman spectrum on the frequency resolution of the spectrum analyzer is investigated. There is a certain value of the resolution of the spectrum analyzer, in which the value of the relative root mean square deviation of the equivalent frequency of the anti-Stokes component of the Raman spectrum is practically not reduced. This allows you to select a spectra analyzer with optimum characteristics for a temperature measurement tool that is built on the effect of Raman.

6 References

1. Kryvenchuk Yu., Shakhovska N., Vovk O., Melnikova N. Computer Simulation of Functions of Transformation of Optical Circuits of Measurement of Temperature Based on Raman Effect and Structure of Algorithm for Their Study. Radioelektronika, Informatika, management. № 3 (46). p. 25–33. (2018)
2. Timans P.J., McMahon R., Ahmed H., Hopper G.F.: Temperature distributions and molten zones induced by heating with line-shaped electron beams. Appl. Phys. 66, 6, 2285. (1989)
3. Melnykova N., Marikutsa U., Kryvenchuk U. The new approaches of heterogeneous data consolidation. p. 408–411. (2018)
4. Korzh R., Fedushko S., Trach O., Shved L., Bandrovskyi H.: Detection of department with low information activity. Proceedings of the XIth International Scientific and Technical Conference "Computer Sciences and Information Technologies". pp. 224-227. (2017)
5. Arzubov M., Shakhovska N., Lipinski P.: Analyzing ways of building user profile based on web surf history. 12th International Scientific and Technical Conference on Computer Sciences and Information Technologies (CSIT). p. 377-380. (2017)
6. Subbarao E.: An Overview. in Advances in Ceramics: Science and Technology of Zirconia, Eds. A.H. Heuer, L.W. Hobbs. American Ceramic Society, pp. 1-24. (1981).
7. Shakhovska N. Consolidated processing for differential information products. Perspective Technologies and Methods in MEMS Design. p. 176-177. (2011)
8. Patil R.N., Subbarao E.C.: Monoclinic-Tetragonal Phase Transition in Zirconia: Mechanism, Pretransformation and Coexistance . Acta Cryst. p. 535-542. (1970)
9. Kryvenchuk, Y., Shakhovska, N., Shvorob, I., Montenegro, S., Nechepurenko, M.: The Smart House based System for the Collection and Analysis of Medical Data. CEUR, Vol-2255. pp 215- 228. (2018).

10. Quintard P., Barberis P., Mirgorodsky A., Merle-Mejean T.: Comparative Lattice-Dynamical Study of the Raman Spectra of Monoclinic and Tetragonal Phases of Zirconia and Hafnia. J. Am. Ceram. Soc. pp. 1745- 1749. (2002).
11. Kryvenchuk, Y., Shakhovska, N., Melnykova, N., & Holoshchuk, R.: Smart Integrated Robotics System for SMEs Controlled by Internet of Things Based on Dynamic Manufacturing Processes. Springer, Cham. pp. 535-549. (2018).
12. Syerov Yu., Fedushko S., Loboda Z.: Determination of Development Scenarios of the Educational Web Forum. Proceedings of the XIth International Scientific and Technical Conference. pp. 73-76. (2016).
13. Duc Huy L., Laffez P., Daniel P., Jouanneaux A., The Khoi N., Simeone D.: Structure and phase component of ZrO2 thin films studied by Raman spectroscopy and X-ray diffraction. Mater. Sci. Eng. B, 104, pp. 163-168 (2003).
14. Stetsyshyn Y., Awsiuk K., Kusnezh V., Raczkowska J., Jany B., Kostruba A., Harhay K., Ohar H., Lishchynskyi O., Shymborska Y., Kryvenchuk Y., Krok F., Budkowski A. Shape-controlled synthesis of silver nanoparticles in temperature-responsive grafted polymer brushes for optical applications. Applied Surface Science. 463.p. 1124–1133. (2018).
15. Yashima M. and et. al.: Determination of teteragonal-cubic phase boundary of Zr1-XRXO2-X/2 (R = Nd, Sm, Y, Er and Yb) by Raman scattering. J. Phys. Chem. Solids, 57, pp. 17-24. (1996).
16. Tsmots I., Skorokhoda O., Tsymbal Yu., Tesliuk T., Khavalko V.: Neural-Like Means for Data Streams Encryption and Decryption in Real Time. In: IEEE Second International Conference on Data Stream Mining & Processing. pp.438-443 (2018).
17. Tsmots I., Teslyuk V., Batyuk A., Khavalko V., Mladenow A.: Information-Analytical Support to Medical Industry. In: CEUR, vol.2488, p. 246- 257 (2019)
18. Fedushko S., Syerov Yu. (2020) Classification of Medical Online Helpdesk Users. CEUR Workshop Proceedings. 2020. Vol 2544: Proceedings of the International Conference on Rural and Elderly Health Informatics (IREHI 2018). http://ceur-ws.org/Vol-2544/shortpaper6.pdf
19. Fedushko S. (2020) Adequacy of Personal Medical Profiles Data in Medical Information Decision-Making Support System.CEUR Workshop Proceedings. – 2020. Vol 2544: Proceedings of the International Conference on Rural and Elderly Health Informatics (IREHI 2018). http://ceur-ws.org/Vol-2544/shortpaper4.pdf
20. Khavalko V., Tsmots I. Image classification and recognition on the base of autoassociative neural network usage // IEEE 2nd Ukraine Conference on Electrical and Computer Engineering (UKRCON-2019). p. 1118-1121. (2019)
21. Kryvenchuk Y., Boyko N., Helzynskyy I., Helzhynska T., Danel R.: Synthesis control system physiological state of a soldier on the battlefield. CEUR. Vol. 2488. Lviv, Ukraine, p. 297–306. (2019)
22. Boyko N., Pylypiv O., Peleshchak Y., Kryvenchuk Y., Campos J.: Automated document analysis for quick personal health record creation. 2nd International Workshop on Informatics and Data-Driven Medicine. IDDM 2019. Lviv. p. 208-221. (2019)
23. Kryvenchuk Y., Mykalov P., Novytskyi Y., Zakharchuk M., Malynovskyy Y., Řepka M.: Analysis of the architecture of distributed systems for the reduction of loading high-load networks. Advances in Intelligent Systems and Computing. Vol.1080. p.759-550. (2020)
24. Kryvenchuk Y.,Vovk O., Chushak-Holoborodko A., Khavalko V., Danel R.: Research of servers and protocols as means of accumulation, processing and operational transmission of measured information. Advances in Intelligent Systems and Computing. Vol.1080. p.920-934. (2020)